











To cite this article: Koksall M, Ozkan E, Aypa A, Akinci E, Kayaaslan B, Hasanoglu İ, Kaya Kalem A, Eser F, Imamoglu Buyukbayraktar FG, Rahmet Guner H. Classification of thorax CT findings of Covid-19 patients, their correlation with clinical and laboratory data. Turk J Clin Lab 2022; 3: 322-332.

Original Article

Classification of thorax ct findings of Covid-19 patients, their correlation with clinical and laboratory data

Covid-19 pnömonili hastaların toraks BT bulgularının sınıflandırılması, klinik ve laboratuvar verileriyle korelasyonu

Murathan Koksall¹ , Erdem Ozkan*¹ , Adalet Aypak² , Eragul Akinci² , Bircan Kayaaslan^{2,3} , İmran Hasanoglu^{2,3} , Ayse Kaya Kalem^{2,3} , Fatma Eser^{2,3} , Fatma Gul Imamoglu Buyukbayraktar¹ , Hatice Rahmet Guner^{2,3,4} 

¹Ankara City Hospital, Radiology Department, Ankara, Turkey

²Ankara City Hospital, Department of Infectious Diseases, Ankara, Turkey

³Ankara Yıldırım Beyazıt University, Department of Infectious Diseases, Ankara, Turkey

⁴COVID-19 Advisory Committee of the Ministry of Health of Turkey, Turkey

Abstract

Aim: The aim of the study is to classify patients infected with Covid-19 in our population according to the radiological consensus defined by Radiology Society of North America (RSNA) and American College of Radiology (ACR) and to show the relationship of the patients with clinical-laboratory findings.

Material and Methods: 127 cases (74 males, 53 females; age range 19-92 years) who applied to Ankara City Hospital with symptoms such as fever, cough and respiratory distress and whose laboratory findings were compatible with Covid-19 were included in our study. The thorax computed tomography (CT) findings of the cases were classified according to the RSNA criteria and their relationship with clinical-laboratory data was statistically evaluated.

Results: 47.2% of them had fever, 62.2% cough, 22 dyspnea, 4.7% diarrhea and 28.3% fatigue-malaise symptoms. When the thorax CT findings were evaluated, 55% of the patients had a typical appearance, 21% intermediate appearance, 11% atypical appearance and 13% negative appearance.

Conclusion: It is obvious that thoracic CT examination has many advantages in evaluating Covid-19 pneumonia. However, it was concluded that more observations should be made in order to classify the findings better and to reveal their relationship with clinical-laboratory findings.

Keywords: Covid-19, computed tomography, pneumonia

Corresponding Author*: Erdem Ozkan, Ankara City Hospital, Ankara, Turkey

E-mail: erdemozkan5454@gmail.com

ORCID: 0000-0001-8120-7051

Doi: 10.18663/tjcl.1021460

Received: 13.11.2021 accepted: 11.09.2022

Öz

Amaç: Çalışmanın amacı, popülasyonumuzdaki COVID-19 ile enfekte olan hastaları, Kuzey Amerika Radyoloji Derneği (RSNA) ve Amerikan Radyoloji Koleji (ACR) tarafından tanımlanan radyolojik konsensusa göre sınıflandırmak ve hastaların klinik-laboratuvar bulguları ile ilişkisini göstermektir.

Gereç ve Yöntemler: Ankara Şehir Hastanesi'ne ateş, öksürük ve solunum sıkıntısı gibi semptomlarla başvuran ve laboratuvar bulguları Covid-19 ile uyumlu 127 olgu (74 erkek, 53 kadın; yaş aralığı 19-92) dahil edildi. Olguların toraks bilgisayarlı tomografi (BT) bulguları RSNA kriterlerine göre sınıflandırıldı ve klinik-laboratuvar verileriyle ilişkisi istatistiksel olarak değerlendirildi.

Bulgular: Olguların % 47,2'sinde ateş,% 62,2 öksürük, 22 nefes darlığı,% 4,7 ishal ve% 28,3 yorgunluk-halsizlik semptomları vardı. Toraks BT bulguları değerlendirildiğinde hastaların % 55'inde Covid-19 pnömonisi açısından tipik görünüm,% 21'inde indetermine görünüm,% 11'inde atipik görünüm ve% 13'ünde negatif görünüm vardı.

Sonuçlar: Toraks BT incelemesinin Covid-19 pnömonisini değerlendirmede pek çok avantajı olduğu aşikardır. Ancak bulguları daha iyi sınıflandırmak ve klinik-laboratuvar bulguları ile ilişkisini ortaya çıkarmak için daha fazla gözlem yapılması gerekmektedir.

Anahtar Kelimeler: COVID-19, bilgisayarlı tomografi, pnömoni

Introduction

The Novel Covid-19 infection, which emerged in Wuhan City, People's Republic of China, in December 2019, and turned into a pandemic in a short time, causing lots of deaths around the world, has been seen in our country as from March. Our knowledge on this new infection process has rapidly increased, however, there are lots of things that we still don't know and have to solve. As we better understand the clinical, laboratory and imaging findings, we can much help patients.

Covid-19 patients typically present with fever, cough, dyspnea and muscle pain [1].The standard diagnosis method is the detection of viral nucleotide by the real-time polymerase chain reaction (RT-PCR) with an oropharyngeal or nasal swab or bronchoalveolar lavage material [1]. However, the current studies show that the sensitivity of RT-PCR ranges from 60% to 71% [2]. On the other hand, it was shown that the thorax CT examination has a sensitivity of 56-98% in the early period of Covid-19 pneumonia [2]. The thorax CT examination shows ground-glass opacities (GGO) and consolidation, which were reported to have shown distribution mostly in lower lobes and peripheral areas [1,3]. However, the described CT findings are non-specific, which emerge due to many infectious and non-infectious factors. This sometimes causes confusion among radiologists as well as clinicians. In this regard, the RSNA and the ACR classified the thorax CT findings of Covid-19 patients a consensus panel [3].

Based on this consensus, the findings were categorized into typical, atypical and negative appearance for pneumonia. This study aimed to classify our patient population based on this

consensus. We aimed to determine the possible relationship between the clinical and laboratory findings of the patients among the classified patient groups.

Material and Methods

Turkish Ministry of Health approval was obtained on 4 May, 2020 and local ethics committee approval was received from Ankara City Hospital Ethical Committee, Turkey (approved number: 84892257-604.01.02-E.14659) on 30 April, 2020. Informed consent was waived due to the retrospective nature of this study.

Cases

127 patients older than 18 years of age, who applied to Ankara City Hospital with symptoms such as fever, cough, and dyspnea in March-June 2020, whose PCR test was positive with the preliminary diagnosis of Covid-19 infection, and whose thorax CT examination was obtained on the day of admission to the hospital, were included in the study.

Patients younger than 18 years of age, who did not have a thorax CT scan performed in our hospital, who had a low quality thorax CT scan that made the evaluation difficult, and whose clinical-laboratory findings could not be reached or were incomplete, were not included in the study.

Imaging Technique

The chest CT examinations were acquired by using 128-slice RevolutionEvo CT (GE Healthcare) scanners in the supine position at full inspiration from lung apices to the inferior level of the costophrenic angle. The acquisition parameters were as follows: 100 or 120 kVp; 80-400 mAs; 1.375, pitch; 0.625 reconstruction

interval; 0.5 seconds (sec) rotation time. Slice thickness was 1.25 mm. Automatic exposure control system (ASiR, GE, Healthcare) regulated the tube current. All chest CT examinations were obtained without intravenous contrast material.

Imaging and Clinical Interpretation

The radiological findings were evaluated and classified by experienced thoracic radiologists based on the RSNA and ACR criteria. The clinical examination, follow-up and laboratory tests were performed and documented by the infectious diseases clinic.

Statistical Analysis

The data were evaluated by using SPSS statistical package program version 25 (IBM Corp. Released 2017. IBM SPSS Statistics for Windows, Version 25.0. Armonk, NY: IBM Corp.). Descriptive statistics of categorical and continuous variables are expressed as mean, \pm SD, median, numbers and percentages. The Levene's test was used to test the homogeneity of variances. Normality of distribution was examined by the "Shapiro-Wilk" test. Binary comparisons were performed by using one-way variance analysis. In multiple comparisons, the Bonferroni-Dunn test was used when appropriate and the Kruskal Wallis test was used when the Bonferroni test was not appropriate. The relationships between categorical variables were analyzed by using Fisher's Exact Test and Chi-Square test. Logistic regression analysis was performed to determine risk factors in patients and the results are presented with Odds Ratio and 95% confidence intervals. A level of $p < 0.05$ and $p < 0.01$ was considered statistically significant.

Results

The age of 127 patients included in the study ranged from 19 to 92, and the average age of them was 50.5 years. Patients younger than 18 year old and with significant artifacts on thoracic CT scans were excluded from the study. 42% (n=53) of the patients were women, 59% (n=74) were men. 47.2% of them had fever, 62.2% cough, 22 dyspnea, 4.7% diarrhea and 28.3% fatigue-malaise symptoms.

87% (n=111) of the patients responded to conventional Covid-19 treatment, while 13% did not respond to the treatment and advanced treatment methods such as anti-interleukin, for which plasma treatment were attempted. 17% (n=22) of the patients needed to intensive care treatment. 5% (n=7) of the cases died in follow up.

When the thorax CT findings were evaluated, 55% of the patients had a typical appearance, 19% intermediate appearance, 11% atypical appearance and 15% negative appearance. The findings are summarized in table 1.

Table 1. Distribution of the types

	n	(%)
Typical	70	%55,1
Indeterminate	24	%18,9
Atypical	14	%11,0
Negative	19	%15,0

56% of the GGO and consolidations showed peripheral-subpleural distribution, 3.9% central-perihilar, 20.8% diffuse and 8.7% random distribution. When the lateralization was examined, unilateral involvement was determined in 30% of the patients, and bilateral involvement was determined in 70% of them. 18.1% of the patients had a single lesion, while 8% had a few lesions (up to 5), 36.2% multiple lesions, 21.3% diffuse or confluence infiltration. The findings are summarized in tables 2 and 3.

Table 2. Axial findings of involvement

		n	(%)
Peripheral	No	55	%43,3
	Yes	72	%56,7
Random	No	116	%91,3
	Yes	11	%8,7
Diffuse	No	112	%88,2
	Yes	15	%11,8
Central	No	122	%96,1
	Yes	5	%3,9

Table 3. Lateralization findings

		n	(%)
Unilateral	No	95	%74,8
	Yes	32	%25,2
Bilateral	No	58	%45,7
	Yes	69	%54,3

91 patients (72% of the patients) had GGO. 14% (n=18) of the patients had consolidation only. 53.5% of the patients had CPA accompanying GGO and consolidation, 7.9% reversed halo sign, 26% halo, 7.1% air bronchogram, 37% vascular enlargement, 33% bronchial enlargement and bronchial wall thickening, 10% air bubble, 4.7% centrilobular nodules, 1.4% tree-in-bud appearance, 1.6% pericardial fluid, 20% moderate lymph node enlargement, 11.5% perilobular involvement, and 7.7% pleural effusion or thickening (figures 1-4). In 21.5% of the patients, linear or reticular densities were observed in the subpleural area.

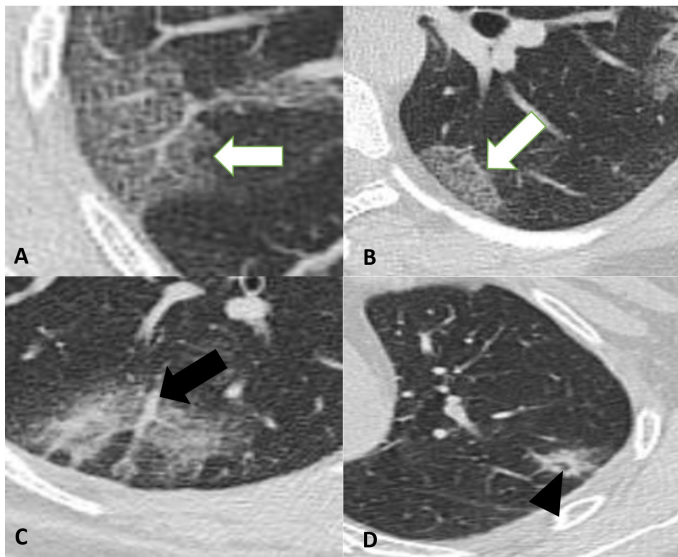


Figure 1. Crazy-paving pattern (white arrow, **A** and **B**), vascular enlargement (black arrow, **C**) and air bubble (arrowhead, **D**).



Figure 2. 48-year-old woman who presented with productive cough, fatigue and myalgia for six days. Initial CT images obtained show small round areas of mixed ground-glass opacity and consolidation (arrow) (reversed halo sign).

The relationships between the patient types and response to the treatment are summarized in table 4. We found statistically significant relationships between patient types and response to treatment ($\chi^2 = 9.195$, $p < 0.05$, $V = 0.228$) and need for intensive care ($\chi^2 = 8.779$, $p < 0.05$, $V = 0.241$), whereas we found no relationship between the patient types and mortality.

The relationships between CT findings according to patient types and RSNA categories are summarized in table 5.

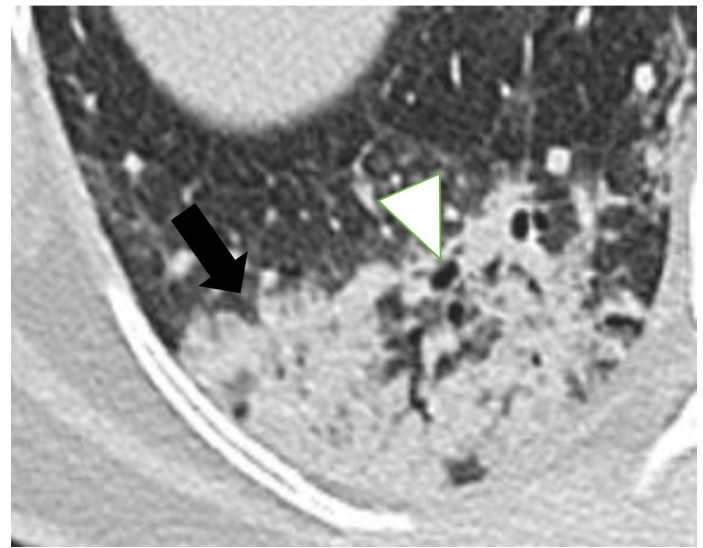


Figure 3. 53-year-old woman with confirmed coronavirus disease (Covid-19). Patient had fever and cough. Consolidation (black arrow) and bronchial changes (arrowhead) are seen in the lower lobe of the right lung

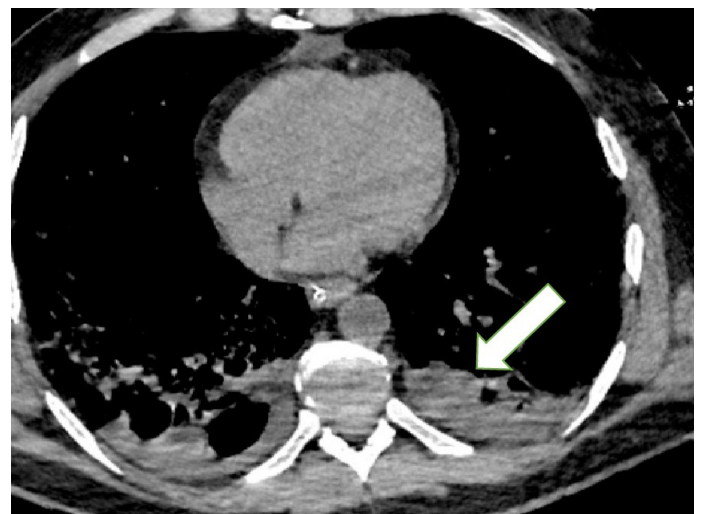


Figure 4. 60-year-old man with laboratory confirmed coronavirus disease (Covid-19). Patient presented with dyspnea for two days. Bilateral pleural effusion is seen on axial CT image (arrow).

When we examined the relationship between the patient types and axial distribution of involvement (i.e. peripheral, central, diffuse, and random involvement), and lobar distribution of involvement (i.e. upper lobe, middle lobe, lower lobe, and all lobes), we found significant relationships between the patients types and peripheral involvement ($\chi^2 = 29.287$, $p < 0.05$, $V = 0.480$); random involvement ($\chi^2 = 9.322$, $p < 0.05$, $V = 0.245$), and diffuse involvement ($\chi^2 = 10.558$, $p < 0.05$, $V = 0.288$), respectively. The relationships between the patient types and distributions of involvement are shown in tables 6 and 7.

Table 4. The relationship between response to treatment and the types

		Typical	Indeterminate	Atypical	Negative	Critical value	Cremer V
		n (%)	n (%)	n (%)	n (%)	(p value)	
Response to treatment	No	13 (18,6%)	1 (4,2%)	2 (14,3%)	0 (0%)	9195 (0,027)*	0,228
	Yes	57 (81,4%)	23 (95,8%)	12 (85,7%)	19 (100%)		
Intensive Care Unit	No	53 (75,7%)	23 (95,8%)	11 (78,6%)	18 (94,7%)	8779 (0,032) *	0,241
	Yes	17 (24,3%)	1 (4,2%)	3 (21,4%)	1 (5,3%)		
ICU survival	Exitus	6 (8,6%)	1 (4,2%)	0 (0%)	0 (0%)	3267 (0,352)	0,160
	Alive	64 (91,4%)	23 (95,8%)	14 (100%)	19 (100%)		

Table 5. The relationship between CT findings and the types

Findings		Typical	Indeterminate	Atypical	Negative	Critical value	Cremer V
		n (%)	n (%)	n (%)	n (%)	(p value)	
Ground-glass opacity	No	0 (0%)	4 (16,7%)	14 (100%)	18 (94,7%)	105924 (001)**	0,913
	Yes	70 (100%)	20 (83,3%)	0 (0%)	1 (5,3%)		
Crazy-paving appearance	No	12 (17,1%)	16 (66,7%)	12 (85,7%)	19 (100%)	58695 (0,001)**	0,680
	Yes	58 (82,9%)	8 (33,3%)	2 (14,3%)	0 (0%)		
Consolidation	No	54 (77,1%)	24 (100%)	12 (85,7%)	19 (100%)	11441 (0,010)**	0,300
	Yes	16 (22,9%)	0 (0%)	2 (14,3%)	0 (0%)		
Reversed halo	No	62 (88,6%)	21 (91,3%)	14 (100%)	19 (100%)	4031 (0,258)	0,179
	Yes	8 (11,4%)	2 (8,7%)	0 (0%)	0(0%)		
Halo	No	45 (64,3%)	17 (70,8%)	13 (92,9%)	19 (100%)	12827 (0,005)**	0,318
	Yes	25 (35,7%)	7 (29,2%)	1 (7,1%)	0 (0%)		
Tree in buds	No	70 (100%)	24(100%)	12 (85,7%)	19 (100%)	16401 (0,001)**	0,359
	Yes	0 (0%)	0 (0%)	2 (14,3%)	0 (0%)		
Air between bronchograms	No	64 (91,4%)	24 (100%)	11 (78,6%)	19 (100%)	7888 (0,048) *	0,249
	Yes	6 (8,6%)	0 (0%)	3 (21,4%)	0 (0%)		
Vascular changes	No	27 (38,6%)	21 (87,5%)	13 (92,9%)	19 (100%)	40610 (0,001)**	0,565
	Yes	43 (61,4%)	3 (12,5%)	1 (7,1%)	0 (0%)		
Bronchial changes	No	34 (48,6%)	21 (87,5%)	11 (78,6%)	19 (100%)	25492 (0,001)**	0,448
	Yes	36 (51,4%)	3 (12,5%)	3 (21,4%)	0 (0%)		
Air bubbles	No	58 (82,9%)	24 (100%)	13 (92,9%)	19 (100%)	8683 (0,034) *	0,261
	Yes	12 (17,1%)	0 (0%)	1 (7,1%)	0 (0%)		
Subpleural reticulations	No	46 (65,7%)	23 (95,8%)	14 (100%)	19 (100%)	21183 (0,001)**	0,408
	Yes	24 (34,3%)	1 (4,2%)	0 (0%)	0 (0%)		
Pleural changes	No	63 (90%)	23 (100%)	13 (92,9%)	19 (100%)	4431 (0,218)	0,188
	Yes	7 (10%)	0(0%)	1 (7,1%)	0 (0%)		
Centrilobular nodule	No	69 (98,6%)	24 (100%)	9 (64,3%)	19 (100%)	33692 (0,001)**	0,515
	Yes	1(1,4%)	0 (0%)	5 (35,7%)	0 (0%)		
Lymphadenopathy	No	47 (67,1%)	23(95,8%)	13 (92,9%)	19 (100%)	17388 (0,001)**	0,370
	Yes	23 (32,9%)	1(4,2%)	1(7,1%)	0 (0%)		
Pericardial changes	No	69 (98,6%)	23(100%)	14 (100%)	19 (100%)	0,806 (0,848)	0,080
	Yes	1 (1,4%)	0 (0%)	0 (0%)	0 (0%)		
Perilobular involvement	No	57 (81,4%)	23(95,8%)	14 (100%)	19 (100%)	9305 (0,026) *	0,271
		13 (18,6%)	1 (4,2%)	0 (0%)	0 (0%)		

**p<0,01 *p<0,05 ψ Pearson's Chi-square Test

When we compared RSNA categories and laboratory findings with the Spearman correlation test, we found statistically significant differences between the patient types in terms of lymphocyte, neutrophil / lymphocyte ratio, C-reactive protein, myoglobin, ferritin, and D-dimer variables (p <0.05 for all). The

mean levels of ferritin and D-dimer were significantly higher in the typical group compared to the other three groups. The comparison of patient types according to laboratory findings are summarized in table 8.

Table 6. The relationship between axial involvement findings and the types

		Typical n (%)	Indeterminate n (%)	Atypical n (%)	Negative n (%)	Critical value (p value)	Cremer V
Peripheral	No	23 (32,9%)	8 (33,3%)	5 (35,7%)	19 (100%)	29287 (0,001) **	0,480
	Yes	47 (67,1%)	16 (66,7%)	9 (64,3%)	0 (0%)		
Random	No	64 (91,4%)	19 (79,2%)	14 (100%)	19 (100%)	9322 (0,025) *	0,245
	Yes	6 (8,6%)	5 (20,8%)	0 (0%)	0 (0%)		
Diffuse	No	56 (80%)	24(100%)	13(92,9%)	19(100%)	10558 (0,014) *	0,288
	Yes	14 (20%)	0 (0%)	1 (7,1%)	0 (0%)		
Central	No	69(98,6%)	22 (91,7%)	12(85,7%)	19(100%)	7134 (0,068)	0,237
	Yes	1 (1,4%)	2 (8,3%)	2 (14,3%)	0 (0%)		

**p<0,01 *p<0,05 ψ Pearson's Chi-square test

Table 7. The relationship between lobar involvement findings and the types

		Typical n (%)	Indeterminate n (%)	Atypical n (%)	Negative n (%)	Critical value (p value)	Cremer V
Upper	Yes	66 (94,3%)	20 (83,3%)	11 (78,6%)	19 (100%)	7997 (0,046) *	0,241
	No	4 (5,7%)	4 (16,7%)	3 (21,4%)	0 (0%)		
Medial	Yes	68 (97,1%)	19 (79,2%)	9 (64,3%)	19 (100%)	20461 (0,001) **	0,401
	No	2 (2,9%)	5 (20,8%)	5 (35,7%)	0 (0%)		
Lower	Yes	59 (84,3%)	9 (37,5%)	8 (57,1%)	19 (100%)	29775 (0,001) **	0,484
	No	11 (15,7%)	15 (62,5%)	6 (42,9%)	0 (0%)		
Total	Yes	16 (22,9%)	21 (87,5%)	14 (100%)	19 (100%)	66495 (0,001) **	0,724
	No	54 (77,1%)	3 (12,5%)	0 (0%)	0 (0%)		

**p<0,01 *p<0,05 ψ Pearson's Chi-square test

Table 8: The relationship between laboratory findings and the types

Laboratory findings	Typical	Indeterminate	Atypical	Negative	Critical value
	Mean ±SD [Median]	Mean ±SD [Median]	Mean ±SD [Median]	Mean ±SD [Median]	(p)
Neutrophile (10 ⁹ /L)	4666,86±2948,3 [3960]	3705,00±2271,77 [3015]	4465,71±2285,99 [3880]	3640,00±1583,40 [3400]	7341 (0,062) ψ
Lymphocyte (10 ⁹ /L)	1179,71±594,08 [1070] a	1616,67±1071,26 [1490] b	1552,14±754,14 [1520] ab	1315,26±688,69 [1300] ab	8939 (0,030) ψ *
Neutropile /Lymphocyte	5,54±6,87 [3,42] a	3,95±2,05 [2,05] b	2,68±1,92 [2,13] b	3,81±3,12 [2,45] ab	12241 (0,007) ψ **
C-reactive protein (g/L)	0,06±0,07 [0,02] a	0,03±0,05 [0] b	0,03±0,03 [0,01] b	0,01±0,01 [0] ab	19768 (0,001) ψ **
Myoglobin (µg/L)	82,40±141,86 [47,50] a	65,52±75,31 [35] a	26,25±10,36 [27] b	65,47±128,83 [32] b	9777 (0,021) ψ *
Ferritin (µg/L)	349,44±339,41 [287] a	208,50±243,47 [88] b	137,57±118,15 [120,50] b	162,50±149,58 [95] b	11561 (0,009) ψ **
D-dimer (mg/L)	1,06±2,22 [0,58] a	0,85±1,07 [0,34] b	0,54±0,39 [0,44] b	0,95±2,17 [0,24] b	10622 (0,014) ψ *
IL-6 (pg/mL)	43,25±89,80 [19,10]	32,43±69,47 [11,85]	105,65±297,17 [5,28]	9,25±8,52 [5,87]	7565 (0,056) ψ

**p<0,01

*p<0,05

Δ One way variance analysis (ANOVA); ψ Kruskal Wallis Test;

a, b, : Different letters in the same column represent a statistically significant difference (p<0.05).

When the relationships between symptoms and types were examined, statistically significant relationships were found between dyspnea and the patient types ($\chi^2= 11,677, p <0.05, V = 0.303$). The findings are shown in table 9.

We created a model between CT findings and RSNA categories by using the multinomial logistic regression method. For this

purpose, we used the predictive ability of 12 CT findings including peripheral-perilobular distribution, bilateral involvement, involvement of all lobes, diffuse involvement, GGO, CPA, halo sign, vascular changes, bronchial changes, subpleural reticular-linear densities, and centrilobular nodules. The findings are summarized in tables 10 and 11.

Table 9: The relationship between the symptoms and the types

		Typical n (%)	Indeterminate n (%)	Atypical n (%)	Negative n (%)	Critical value (p value)	Cremer V
Fever	Yes	33 (47,1%)	11 (45,8%)	8 (57,1%)	8 (42,1%)	0,771 (0,856)	0,078
	No	37 (52,9%)	13 (54,2%)	6 (42,9%)	11 (57,9%)		
Chough	Yes	26 (37,1%)	8 (33,3%)	5 (35,7%)	9 (47,4%)	0,982 (0,806)	0,088
	No	44 (62,9%)	16 (66,7%)	9 (64,3%)	10 (52,6%)		
Dyspnea	Yes	49 (70%)	23 (95,8%)	9 (64,3%)	18 (94,7%)	11677 (0,009) **	0,303
	No	21 (30%)	1 (4,2%)	5 (35,7%)	1 (5,3%)		
Diarrhea	Yes	67 (95,7%)	22 (91,7%)	13 (92,9%)	19 (100%)	1848 (0,604)	0,121
	No	3 (4,3%)	2 (8,3%)	1 (7,1%)	0 (0%)		
Fatigue	Yes	49 (70%)	18 (75,0%)	11 (78,6%)	13 (68,4%)	0,654 (0,884)	0,072
	No	21 (30%)	6 (25,0%)	3 (21,4%)	6 (31,6%)		

**p<0,01 *p<0,05 ψ Pearson Chi-square test

Table 10: The results of logistic regression model for the categories

Category	Parameter	β coefficient	SE	p	Odds Ratio (CI)	Model meaningfulness
Typical (Model 1)	Constant	0,821	0,410	0,045 *	2,272	2 Log likelihood=70,497 Cox & Snell R Square=0,562 Nagelkerke R Square=0,751 =104,924 p=0,001 **
	Bilateral	2,209	0,695	0,001 **	9,106 (2,332-35,554)	
	Lobar-total	2,574	0,797	0,001 **	13,115 (2,750-62,555)	
	Vascular change	1,847	0,717	0,010 **	6,343 (1,557-25,844)	
Indeterminate (Model 2)	Constant	-2,178	0,365	0,001 **	0,113	-2 Log likelihood= 104,448 Cox & Snell R Square=0,191 Nagelkerke R Square=0,297 = 26,966 p=0,001 **
	Lobar-total	-2,417	0,778	0,002 **	0,089 (0,019-0,410)	
	GGO	1,780	0,614	0,004 **	5,929 (1,781-19,740)	
	Bilateral	-0,877	0,684	0,200	0,416 (0,109-1,589)	
Atypical (Model 3)	Constant	-2,810	0,631	0,001 **	0,060	-2 Log likelihood= 56,060 Cox & Snell R Square=0,223 Nagelkerke R Square=0,446 = 32,080 p=0,001 **
	GGO	-3,316	1,115	0,003 **	0,036 (0,004-0,323)	
	Crazy pavement	-1,477	1,153	0,200	0,228 (0,024-2,188)	
Negative (Model 4)	Constant	-1,825	0,309	0,001 **	0,161	-2 Log likelihood= 79,910 Cox & Snell R Square=0,146 Nagelkerke R Square=0,268 = 20,079 p=0,001 **
	GGO	-2,509	0,618	0,001 **	0,081 (0,024-0,273)	

**p<0,01 *p<0,05 GGO: Ground-glass opacity

Table 11: Classification chart for the categories

Category			Expected		Accuracy ratios
			No	Yes	
Typical (Model 1)	Observed	No	55	4	93,2
		Yes	9	59	86,8
	Overall Percentage				89,8
Indeterminate (Model 2)	Observed	No	92	8	92,0
		Yes	15	12	44,4
	Overall Percentage				81,9
Atypical (Model 3)	Observed	No	113	0	100,0
		Yes	14	0	0,0
	Overall Percentage				89,0
Negative (Model 4)	Observed	No	110	0	100,0
		Yes	17	0	0,0
	Overall Percentage				86,6

We created 44 logistic regression models for typical, indeterminate, atypical and negative groups. In model 1, there is a statistically significant relationship between the typical group and “Bilateral Involvement (BI)”, “Involvement of All Lobes (IAL)”, and “Vascular Changes (VC)” ($\chi^2 = 104.924$, $p < 0.05$). Cox & Snell R Square and Nagelkerke R Square values represent the variance in the dependent variable explained by the logistic model. Among these values, the Cox & Snell R Square value shows that the model explained 56% and the Nagelkerke R Square value explains 75% of the variance in the dependent variable. When the data about the coefficients of the model is examined, it is seen that the model 1 is as follows:

$$\text{Model 1} = 0.821 + 2.209 (\text{BI}) + 2.574 (\text{IAL}) + 1.847 (\text{VC})$$

When the odds value for model 1 is examined, it is seen that typical category disappearance is 9,106 times higher in the group with no CT compared to the group with CT. Similarly, the typical category disappearance is 13,115 times higher in the group without IAL compared to the group with IAL. Finally, the typical category disappearance is 6.334 times higher in the group without VC compared to the group with VC.

When model 2 is examined, it is seen that there is a statistically significant relationship between the indeterminate category and IAL and GGO (ground glass opacity) parameters ($\chi^2 = 26.966$, $p < 0.05$). The Cox & Snell R Square value shows that the model created explains 19% and the Nagelkerke R Square value explains 30% of the variance in the dependent variable. When the data about the coefficients of the model is examined, it is seen that the model 2 is as follows:

$$\text{Model 2} = -2,178 - 2,417 (\text{IAL}) + 1,780 (\text{GGO}) - 0,877 (\text{BI})$$

When the odds value for model 2 is examined, it is seen that

disappearance of the indeterminate category decreases by 9% in the group without IAL compared to the group with IAL. Similarly, the indeterminate category disappearance is 5,929 times higher in the group without GGO compared to the group with GGO.

When model 3 is examined, it is seen that there is a statistically significant relationship between the atypical category and GGO and the crazy-paving appearance (CPA) parameters ($\chi^2 = 32,080$, $p < 0,05$). The Cox & Snell R Square value shows that the model created explains 22% and the Nagelkerke R Square value explains 45% of the variance in the dependent variable. When the data about the coefficients of the model is examined, the model created is as follows:

$$\text{Model 3} = -2,810 - 3,316 (\text{GGO}) - 1,477 (\text{CPA})$$

When the odds value for model 3 is examined, it is seen that atypical category disappearance decreases by 4% in the group without GGO compared to the group with GGO. Similarly, disappearance of atypical category decreases by 45% in the group without CPA compared to the group with CPA.

When model 4 is examined, it is seen that there is a statistically significant relationship between negative category and the GGO parameter ($\chi^2 = 20.079$, $p < 0.05$). The Cox & Snell R Square value shows that the model created explains 15% and the Nagelkerke R Square value explains 27% of the variance in the dependent variable. When the data about the coefficients of the model is examined, the model created is as follows:

$$\text{Model 4:} \ln(P/1-P) = \ln(\text{odds}) = -1,825 - 2,509 (\text{GGO})$$

When the odds value is examined in model 4, it is seen that the negative category disappearance decreases by 8% in the group without GGO compared to the group with GGO.

The estimated values and real values of the model created are shown in table 12. When the model 1 is examined, it is seen that the model created by logistic regression correctly predicts the typical category with a ratio 89.8%. The model estimates typical disappearance at 93.2% and existence at a ratio of 86.8%.

When model 2 is examined, it is seen that the model created by logistic regression correctly predicts the disappearance of uncertain category with a ratio of 81.9%. The model predicts disappearance of indeterminate category correctly with a ratio of 92% and existence with a ratio of 44.4%.

When model 3 is examined, it is seen that the model created by logistic regression correctly predicts the disappearance of atypical category with a ratio of 89%. It is seen that the model predicts the disappearance of atypical category with a ratio of 100% and existence with a ratio of 0%.

Discussion

As is known, when a thorax CT examination is reported, an algorithm is established over some elementary lesions and patterns. For example, ground-glass opacities, consolidation areas, tree-in-bud appearance, centrilobular nodules, etc. It is also important to be able to identify these patterns and lesions and to determine axial and longitudinal distribution of the lesions, in terms of diagnosis. The radiologist will blend the identified information along with his/her clinical and laboratory knowledge and eventually submit it as a pre-diagnosis to the clinician. The identification and classification of dominant pattern and elementary lesions is also important for the differential diagnosis of Covid-19 pneumonia. In this regard, a common language among radiologists, reducing confusion, is very important in both communication between radiologists and clinicians and in the evaluation of control CT examination results. Many radiology associations carried out studies to establish this common language and identified the most possible pattern and lesions for Covid-19 pneumonia.

When we examined the relationship between the RSNA categories and the BT findings: the typical category was found to be most strongly associated with many CT findings including GGO, CPA and vascular enlargement (figure 5, 6). This means that we may see a wide range of CT findings in the typical category. This may sometimes cause confusion. However, considering the mostly associated findings such as GGO, CPA, peripheral, bilateral involvement, we think that this would significantly decrease our margin of error.

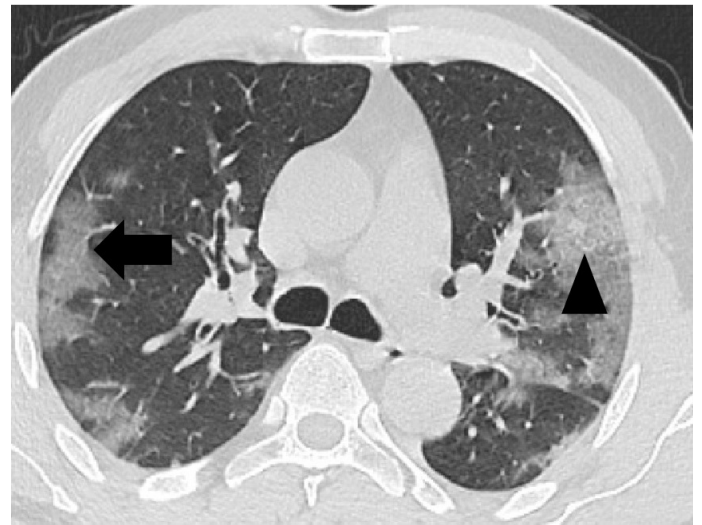


Figure 5. Multiple patchy ground-glass opacities (arrow) and intralobular septal thickening (arrowhead) (crazy-paving pattern)

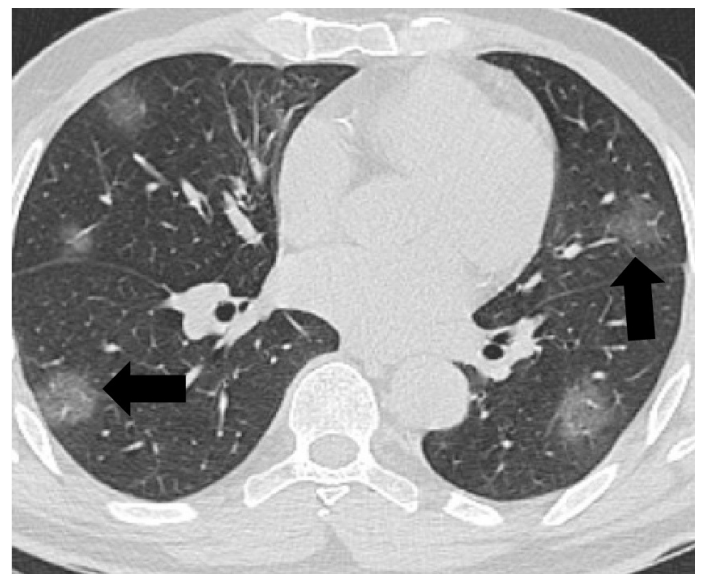


Figure 6. 55-year-old man who presented with chest pain, fever and cough for 3 days. Coronavirus disease (Covid-19) had recently been diagnosed in two of his household members. Axial CT image shows peripheral nodular ground-glass opacities (arrows)

On the other hand, the findings such as lesions with random distribution, unilateral involvement and single or multiple lesions were found to be associated with the intermediate category, and we should cautiously approach Covid-19 diagnosis in the presence of these findings together with GGO or consolidation. Nevertheless, unilateral involvement, involvement of upper-medium lobe, single lesion, tree-in-bud appearance and centrilobular nodule were associated with the typical category, which may detract from Covid-19 diagnosis (figure 7).

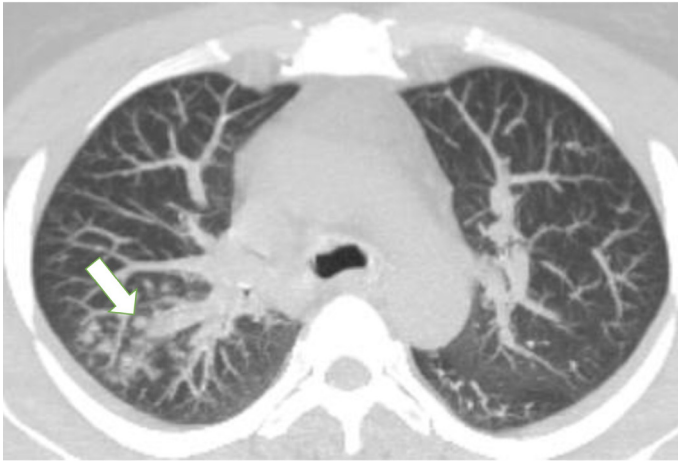


Figure 7. 51-year-old woman who presented with fever and cough for 2 days. CT was performed on day of admission. Axial CT image shows centrilobular nodules in upper lobe of the right lung (arrow). Atypical CT finding for Covid-19 pneumonia

We created models with high accuracy by using the CT findings of our logistic regression study. It is seen that these models give more meaningful results especially for the typical and indeterminate category. We found that the best predictive CT parameters were GGO, CPA, bilateral involvement, and involvement of all lobes. These results suggest that paying particular attention to these 4 parameters is important in guiding us to the correct diagnosis. In addition, these findings are promising in terms of computer-assisted diagnosis in the future. We suggest that, in the future, the improvement of a CAD (computer aided diagnosis) software that can identify lung lesions would have the potential for a diagnosis and categorization with high accuracy.

The early studies on Covid-19 pneumonia revealed that 40 of 41 patients had bilateral involvement and most patients had ground-glass opacities and consolidation [4].

In a prospective case series of 41 patients, CT abnormalities that suggested pneumonia were reported for 100% of the patients. 98% of them showed bilateral lung involvement. The most common CT findings among the patients who applied to intensive care unit were multiple lobar and posterior segmental consolidation [5]. In the another study, Chung et al. show that, the most commonly involved lung was the right lower lobe (76%), while the least commonly involved lung was the right middle lobe (57%) [6].

In another study with 51 patients with confirmed Covid-19, 1324 lung lesions were determined in thorax CT for 1-14 days (4 days on average) as from the onset of symptoms [7].

Jin et al. described typical and atypical thorax CT patterns.

Bilateral, fuzzy-edged intralobular septal thickenings with high density were reported as typical findings in 54.2% of the patients, while multiple irregular consolidative opacities were seen in 31% of the patients. They found atypical findings such as bronchial wall thickening, pleural effusions, LAP and halo sign in nearly 7% of the patients [8].

As can be seen in the studies above, CT findings frequently vary. However, bilateral, lower-lobe, peripheral-peribronchovascular involvement, GGO opacities and accompanying consolidations and crazy-paving appearance were the most commonly seen findings in all the studies.

When the categories were compared by response to treatment, need for intensive care and mortality rates, as can be expected, the most frequent need for intensive care and the highest mortality rate were seen in the typical category. On the other hand, the rate of patients who responded to conventional treatment and showed clinical improvement was 100% in the negative group, 85% in the atypical group, 95% in the intermediate group and 80% in the typical group. As can be seen, since the typical category had the most symptoms as well as a highly intensive care rate and a high mortality rate, however, the lowest rate of response to treatment, it can be said that it was the riskiest group in terms of clinical course.

When the laboratory findings of the cases were evaluated, CRP, myoglobin, ferritin, IL-6 and D-dimer values were found apparently high. There was usually a positive (except for lymphocyte) between the laboratory data and the typical patient category, while a weak but negative correlation was observed between many laboratory parameters and the negative patient category. This suggested that there may be a relationship between the patient RSNA categories and the laboratory findings, and that, as with the clinical data, the highest results may be seen in the typical category.

Conclusion

The benefits of thorax CT examination to evaluate Covid-19 pneumonia are undeniable. We think that the RSNA category will help us in this regard. Nevertheless, more observations are needed to better categorize the findings and to reveal the relationship between clinical presentation and laboratory findings.

Ethics approval

This retrospective study has been approved by the local ethics committee and conducted in accordance with the Declaration of Helsinki (2000).

Declaration of conflict of interest

The authors received no financial support for the research and/or authorship of this article. There is no conflict of interest.

Funding

This research did not receive any specific grant from funding agencies in the public, commercial, or not-for-profit sectors.

References

1. Zhou F, Yu T, Du R et al. Clinical course and risk factors for mortality of adult inpatients with COVID-19 in Wuhan, China: a retrospective cohort study [published correction appears in *Lancet*. 2020 Mar 28;395(10229):1038] [published correction appears in *Lancet*. 2020 Mar 28;395(10229):1038]. *Lancet* 2020;395(10229):1054-1062. doi:10.1016/S0140-6736(20)30566-3.
2. Bai H.X., Hsieh B, Xiong Z et al. Performance of Radiologists in Differentiating COVID-19 from Non-COVID-19 Viral Pneumonia at Chest CT. *Radiology* 2020;296(2):E46-E54. doi:10.1148/radiol.2020200823.
3. Simpson S, Kay FU, Abbara S et al. Radiological Society of North America Expert Consensus Statement on Reporting Chest CT Findings Related to COVID-19. Endorsed by the Society of Thoracic Radiology, the American College of 2019.
4. Chen N, Zhou M, Dong X et al. Epidemiological and clinical characteristics of 99 cases of 2019 novel coronavirus pneumonia in Wuhan, China: a descriptive study. *Lancet* 2020;395(10223):507-513. doi:10.1016/S0140-6736(20)30211-7.
5. Huang C, Wang Y, Li X et al. Clinical features of patients infected with 2019 novel coronavirus in Wuhan, China [published correction appears in *Lancet*. 2020 Jan 30;]. *Lancet* 2020;395(10223):497-506. doi:10.1016/S0140-6736(20)30183-5.
6. Chung M, Bernheim A, Mei X et al. CT Imaging Features of 2019 Novel Coronavirus (2019-nCoV). *Radiology* 2020;295(1):202-207. doi:10.1148/radiol.2020200230.
7. Song F, Shi N, Shan F et al. Emerging 2019 Novel Coronavirus (2019-nCoV) Pneumonia. *Radiology* 2020;295(1):210-217. doi:10.1148/radiol.2020200274.
8. Jin YH, Cai L, Cheng ZS et al. A rapid advice guideline for the diagnosis and treatment of 2019 novel coronavirus (2019-nCoV) infected pneumonia (standard version). *Mil MedRes* 2020;7(1):4. Published 2020 Feb 6. doi:10.1186/s40779-020-0233-6.